International Journal of Mass Spectrometry 289 (2010) 39–46

Contents lists available at ScienceDirect

International Journal of Mass Spectrometry

journal homepage: www.elsevier.com/locate/ijms

Dissociative electron attachment to polyatomic molecules: Ion kinetic energy measurements

Dhananjay Nandi [1], E. Krishnakumar [*,2]

Tata Institute of Fundamental Research, Homi Bhabha Road, Colaba, Mumbai 400005, India

ARTICLE INFO

Article history:
Received 24 August 2009
Received in revised form
20 September 2009
Accepted 21 September 2009
Available online 26 September 2009

Keywords:
Dissociative electron attachment
Negative ion resonance

ABSTRACT

Dissociative electron attachment to SO_2, NO_2, NF_3 and H_2O_2 is studied in terms of the kinetic energies of the dominant fragment ions. The O^- data from SO_2 show that the two major resonances at 4.6 and 7.2 eV respectively have the same dissociation limit. Similarly, the resonances at 1.8 and 3.5 eV in the O^- channel in NO_2 appear to have same dissociation limit of NO ($X\,^2\Pi$) + O^-, while the resonance at 8.5 eV appears to dissociate to give NO ($a\,^4\Pi_i$) along with O^-. We find considerable internal excitation of the neutral fragments in all these cases along with that of NF_3, whereas the negative ion resonance in H_2O_2 appears to fragment almost like a diatomic system with very little internal excitation of the OH and OH^- fragments.

1. Introduction

Dissociative electron attachment (DEA) is a dominant process in low energy inelastic processes in electron–molecule collisions. The resonant electron attachment to molecules and the subsequent decay of the resonance through electron ejection or dissociation leads to the formation of vibrationally and electronically excited molecules, radicals and negative ions, all of which could take part very efficiently in various chemical processes leading to a wide variety of applications. The importance of low energy electrons in inducing chemical reactions has been further enhanced by the potential for chemical control by site/bond selective fragmentation of molecules in DEA [1,2]. In this context, it is important to study the DEA process in individual molecules for the information on the product distributions, their kinetics and the cross-sections. The kinetic energy data of the fragment ions provide important information on the dissociation limits and the internal excitation of the products. The secondary chemical reactions in which the products of the DEA process participate will be crucially dependent on their internal excitation. The kinetic energy data also provide information if the dissociation is a two-body or a three-body process. In this communication, we present measurements of fragment ion kinetic energies from DEA to SO_2, NO_2, NF_3 and H_2O_2 for which very little or absolutely no data exist.

SO_2 and NO_2 are known industrial pollutants and controlling their emission is crucial for protection of the environment. In addition, these are benchmark molecules for studying electron collision from electronically excited molecules. The UV absorption property of SO_2 to form excited states has allowed some of the very first measurements on dissociative electron attachment to electronically excited molecules [3–5]. Similar measurements could be carried out on NO_2 also due to its strong absorption in the visible region. So far there exist no information on the kinetic energy of fragment ions from SO_2 and NO_2 due to DEA.

NF_3 is important as a fluoride source in dry etching applications in semiconductor industry due to its larger cross-section for the production of active radicals as well as in preventing carbonaceous deposits [6,7]. It is also found to be environmentally friendlier as compared to perfluorocarbons like hexafluoroethane and sulphur hexafluoride [8]. Kinetic energy of fragment ions from NF_3 arising from DEA has been measured earlier [9]. However, as discussed later, there appears to be some discrepancy in the results, which we clarify by repeating the measurements.

Hydrogen peroxide is an important minor constituent of earth's atmosphere and its reaction with SO_2 could be the main source of H_2SO_4 in the atmosphere. In addition, H_2O_2 is an agent in the formation of HOx in the troposphere and in the stratosphere [10]. It is also an important molecule in the ozone cycle in the atmosphere as the product of the reaction of O_3 with H_2O. Hydrogen peroxide is important in the radiation damage of biological tissues as it is a product in the radiolysis of water [11]. It is generated by the recombination of hydroxy- radicals formed as one of the primary products of water decomposition by radiation and its behavior towards low energy electrons is directly related to radiation damage of biolog-

* Corresponding author. Fax: +91 22 22804610.
E-mail address: ekkumar@tifr.res.in (E. Krishnakumar).
[1] Currently at Indian Institute of Science Education and Research, Kolkata, India.
[2] Currently on sabbatical at the Open University, Milton Keynes, UK.

1387-3806/$ – see front matter © 2009 Elsevier B.V. All rights reserved.
doi:10.1016/j.ijms.2009.09.009

ical material. Measurements on DEA to H_2O_2 have shown that it has very large cross-sections for the formation of OH and OH^- at very low electron energies [12]. So far there exists no information on the dynamics of the DEA process for this molecule. The kinetic energy data of the fragments is expected to provide some input on this aspect.

2. Experimental

We measure the kinetic energy of the fragment ions using the time-of-flight technique described earlier [13]. The ions produced by the interaction of a pulsed electron beam are extracted into a linear time-of-flight spectrometer of Wiley–McLaren geometry using a small extraction field. The small extraction field and limiting apertures allow only the ions ejected along the flight tube axis and those opposite to it to be detected. The ions ejected in the forward and backward directions to the flight tube axis arrive at the detector with finite time difference, Δt, which is a function of their initial kinetic energy (E_k) and the ion draw out field (E_1), given by the expression [13]

$$\Delta t = \frac{8 \cdot m_i \cdot E_k^{1/2}}{qE_1} \quad (1)$$

where m_i and q are the mass and the charge of ion, respectively.

If the above time difference is large enough, the mass spectrum will show two distinct peaks for a given m_i/q value corresponding to 'direct' and 'turn-around' ions. Using the measured Δt we could obtain the kinetic energy,

$$E_k = \frac{(qE_1 \Delta t)^2}{8m_i} \quad (2)$$

For a decomposition into two fragments, in the centre of mass frame, the total translational energy (E_T) imparted to the fragments can be calculated from the principle of linear momentum conservation as

$$E_T = E_k \cdot \frac{M}{m} \quad (3)$$

where M is the mass of the parent molecule and m is the mass of neutral fragment. For ions with low kinetic energy (<0.1 eV), there is no discrimination against perpendicular velocity component and all the ions are transmitted to the spectrometer and the time-of-flight mass spectra show one peak with fairly Gaussian shape. The average initial kinetic energy can be calculated from full width at half maximum (fwhm), $\Delta t_{1/2}$, of the peak as [14].

$$\overline{E_k} = \frac{(qE_1 \Delta t_{1/2})^2}{3.7m_i} \quad (4)$$

The experimental arrangement used to measure the kinetic energy of the fragment ions resulting from DEA is shown in Fig. 1. A magnetically collimated and pulsed electron beam (pulse width of about 300 ns) is collided at right angles with an effusive molecular beam formed by a capillary array. The magnetic field used for the electron collimation is 50 Gauss. The ions formed by the interaction are extracted at right angles into the linear time-of-flight spectrometer of Wiley–McLaren geometry by a small constant electric field (5 V/cm). We limit the solid angle of detection to a small value by using an aperture of 4 mm diameter at the entrance to the flight tube which is situated at 10 mm from the interaction point and another similar aperture in front of the detector. The detector is a channel electron multiplier operated in the pulse counting mode. The signal from the detector is processed by an amplifier, a constant fraction discriminator and a time to amplitude converter (TAC). The output of the TAC is fed to a pulse height analyzer to obtain the time-of-flight spectrum. The timing signal for starting the TAC is taken

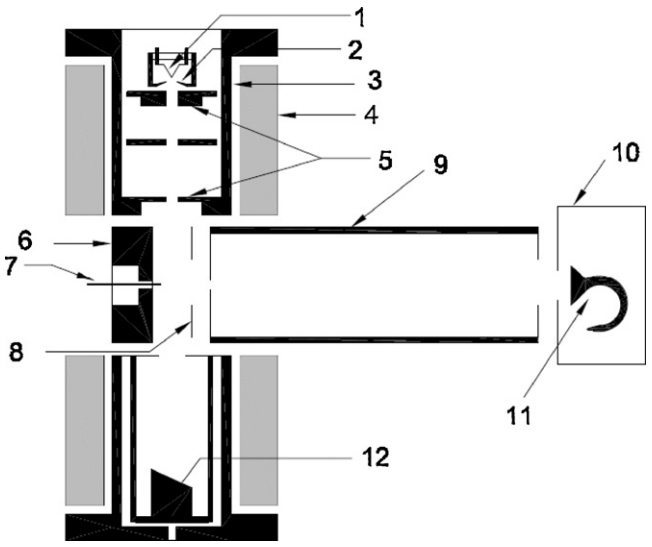

Fig. 1. Schematic of the experimental arrangement. The numbering represents: (1): filament, (2) Pearce element, (3) electron gun housing, (4) magnet coil, (5) electron gun electrodes, (6) pusher electrode, (7) capillary array, (8) puller electrode, (9) flight tube, (10) channeltron housing, (11) channeltron, (12) Faraday cup.

synchronously from the pulse generator that is used for pulsing the electron beam.

We characterized the performance of our spectrometer by measuring the kinetic energy of O^- produced by DEA to O_2 which is well studied. Fig. 2 shows the ion kinetic energy obtained as a function of the electron energy at various points across the resonance which has peak cross-section at 6.5 eV [15]. The results show that the kinetic energy increases with electron energy. An extrapolation of the data points with a straight line intercept at the abscissa should give threshold energy for the reaction, ΔH_0. We find this to be 3.4 eV, which is lower than the expected value of 3.65 eV for O^- from O_2. We also note that the slope of the line is 0.44 as against the expected value of 0.5. These differences may be explained in terms of the finite energy spread of the electron beam. For electron energies below the peak cross-section, the higher energy side of the electron beam will have larger contribution to the ion intensity, whereas at energies above the resonance peak, the lower energy part of the electron beam will have a disproportionate contribu-

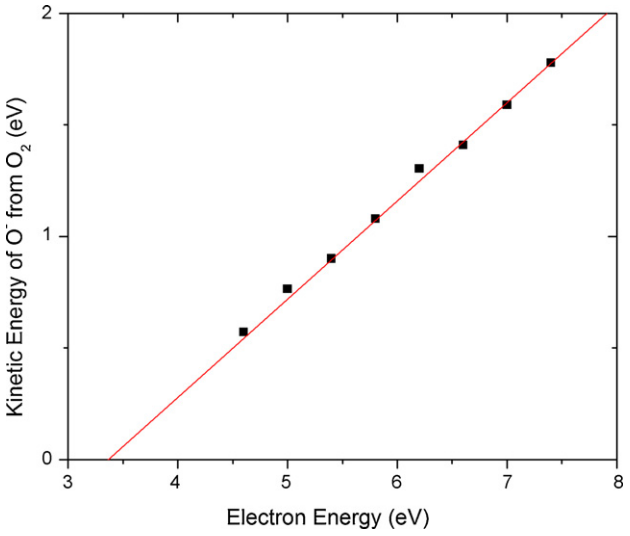

Fig. 2. Measured kinetic energy of O^- from O_2 as a function of electron energy. The straight line through the data points has a slope of 0.44 and intercepts the abscissa at 3.4 eV.

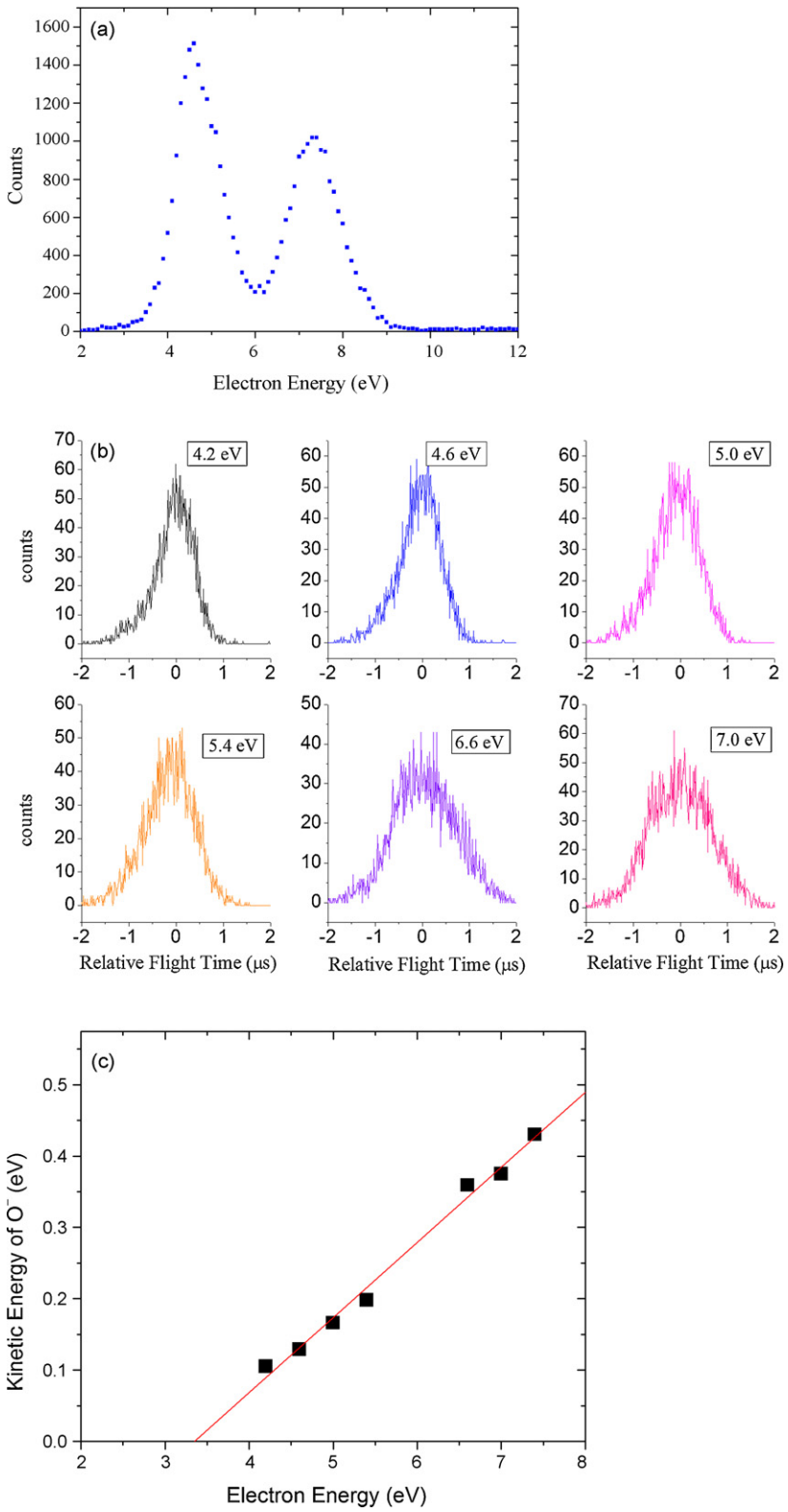

Fig. 3. O^- from DEA to SO_2. (a) ion yield curve, (b) time-of-flight spectra of the ions at various electron energies and (c) measured kinetic energy of the ions as a function of electron energy.

tion to the ion intensity. The effect of this would be to show larger than real kinetic energy for electron energies below the resonance peak and smaller than real kinetic energy for electron energies above the resonance peak. The net effect of these two would be to reduce the slope of the line obtained from ion kinetic energy vs. electron energy graph. This may also lead to a lower value for ΔH_0.

We also note that when the kinetic energy is very small the average energy is computed from the half-width of the single Gaussian peak, given by Eq. (4). This may also have errors due to the thermal spread of the molecular beam. Thus there are limitations in the measurement technique employed in this experiment. However, as we shall show, even with these limitations, new qualitative

information on the DEA to molecules could be obtained with this technique.

3. Results and discussion

3.1. SO_2

The dissociative electron attachment to ground state SO_2 is known to have two major resonances in the energy range of 4–10 eV giving rise to the formation of O^-, S^-, and SO^- at both the resonances [4]. The O^- channel is comparable in intensity at both the resonances, while S^- and SO^- channels are relatively weak at the higher energy resonance. The S^- channel shows a small additional peak at around 9 eV [4]. By comparing the results obtained from DEA to ground and excited states, the two dominant resonances have been identified as $^2A_1$ and $^2B_2$ states, respectively [16].

The ion yield spectrum for the formation of O^- from SO_2 measured in the current experiment is shown in Fig. 3 along with the time-of-flight (ToF) spectra at different electron energies and the measured kinetic energy of the ions. No attempt has been made to measure the kinetic energy of the other fragment ions due to poor statistics. The zero in the *x*-axis (Fig. 3b) refers to an ion with zero velocity along the flight tube axis. In this scale, the 'direct' ions have negative flight times and the 'turn-around' ions have positive ones. The ToF spectra show only one peak, fairly Gaussian in shape, indicating that the ions are produced with very low kinetic energies (comparable to the thermal energy). The width of the ToF spectrum slowly increases with the electron energy. We estimate the kinetic energy of the ions by fitting the curves with a Gaussian and taking the full-width at half maximum (fwhm), $\Delta t_{1/2}$. The kinetic energies are calculated using Eq. (4) and are plotted as a function of the incident electron energy in Fig. 3c. We find that the points covering both the resonances fall on a straight line which has a slope of 0.11 and cuts the *x*-axis at 3.3 eV. Assuming all the excess energy is released as kinetic energy of the fragments, the slope of the straight line would be 0.75. The measured slope of 0.11 indicates that most of the available energy is going into the vibrational, rotational and even electronic (if the $a\,^1\Delta$ state contributes, as discussed below) energy of the SO fragment. A large part of the excess energy going into the vibrational excitation of the SO fragment may indicate that while one of the S–O bond is being broken, the other one is also getting stretched simultaneously. This is consistent with the fact that both the resonances have considerable dissociation probability into the $S^- + O_2$ channel.

The low kinetic energy of the ions indicates that the potential energy surface of the resonance at 4.6 eV has a minimum along the OS–O bond in the Franck–Condon region similar to that given in Fig. 4 for the case of a polyatomic molecule AB. In Fig. 4 we show a schematic of the DEA process in a generic polyatomic molecule AB where both A and B may constitute more than one atom. The vertical dashed lines represent the bounds of the Franck-Condon region. AB^{-*} represents negative ion resonances that dissociate to give fragments A and B^-. The lower resonance has part of its minimum along A–B in the Franck–Condon region, whereas the upper resonance has no minimum in that region. The horizontal line represents the threshold energy at which B^- ions start to form. The ions formed at this energy will have zero kinetic energy and the kinetic energy increases as the electron energy is increased beyond the threshold. However, if the potential energy surface of the resonance is purely repulsive along A–B coordinate or if the potential well does not extend into the Franck–Condon region as shown in the figure for the upper resonance curve, the formation of B^- occurs only at energies well above the threshold. In such a case, the B^- ions will have finite kinetic energy right from the beginning of the ion

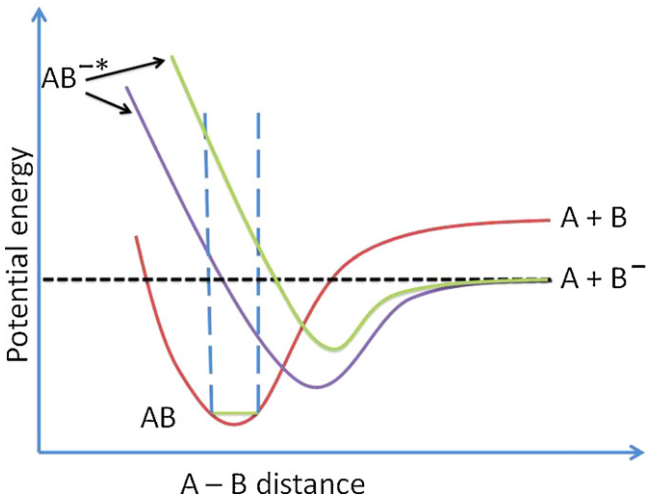

Fig. 4. Schematic of the DEA process in a generic polyatomic molecule AB where both A and B may constitute more than one atom. The vertical dashed lines represent the bounds of the Franck–Condon region. AB^{-*} represents the negative ion resonances which dissociate to give fragments A and B^-. The lower resonance has part of its minimum along A–B in the Franck–Condon region, whereas the upper resonance is entirely repulsive in that region. The horizontal line represents the threshold energy at which B^- is formed.

yield curve. The 4.6 eV resonance in SO_2 may be identified with the lower of the two resonant curves shown in Fig. 4, with a minimum along the OS–O bond and stretching into the Franck–Condon region. On the other hand, we may also conclude that the 7.2 eV resonance is entirely repulsive in the Franck–Condon region. It may be pointed out that one could derive similar information from the ion yield curves if the electron energy resolution is good enough. In such a case the ion yield curve will have a sharp onset right at the threshold energy for its formation if the resonant state is similar to that represented by the lower potential energy curve.

Since the data points corresponding to both the resonances appear to fall on the same straight line as seen in Fig. 3c, we may conclude that both these states have the same dissociation limit. Based on correlation diagrams, these two resonances could have three possible dissociation limits giving O^- [16]. These limits correspond to the formation of SO in the $X\,^3\Sigma^-$, $a\,^1\Delta$ and $b\,^1\Sigma^+$ states. The $a\,^1\Delta$ and $b\,^1\Sigma^+$ states are 0.79 and 1.3 eV respectively higher than the $X\,^3\Sigma^-$ state [17]. Using zero energy ion spectrometry along with a high resolution electron beam, Abouaf and Fiquet-Fayard [18] have shown that the 4.6 eV resonance has some contribution from the SO ($a\,^1\Delta$) limit. We cannot rule out a similar contribution from the SO ($a\,^1\Delta$) limit at the second resonance also. However, we note that the observed heat of formation ($\Delta H_0 = 3.3$ eV) is considerably lower than the expected value of 4.2 eV based on the OS–O bond dissociation energy (5.66 eV) and the electron affinity of O^- (1.46 eV). If SO is formed in the excited $a\,^1\Delta$ state, the value of ΔH_0 would be 4.99 eV. Any substantial contribution from the formation of SO ($a\,^1\Delta$) state is likely to increase the value of ΔH_0 from 4.2 eV, increasing the observed disparity further. Thus, within the experimental uncertainties, our results indicate the dominant dissociation limit in both the resonances to be the $X\,^3\Sigma^-$ limit.

It is not clear if the finite energy spread (~0.5 eV) of the electron beam and the approximation used in Eq. (4) to evaluate the kinetic energy will explain the large shift of ΔH_0 to the lower energy. A possible reason for this is the presence of vibrationally excited molecules in small quantities in the interaction region produced by the radiation from the filament within the electron gun and migrating to the interaction region. We note that the ion yield curve also shows a threshold of about 3.3 eV, similar to previous measurements [4,16]. This trend is seen in the case of NO_2 also, as discussed

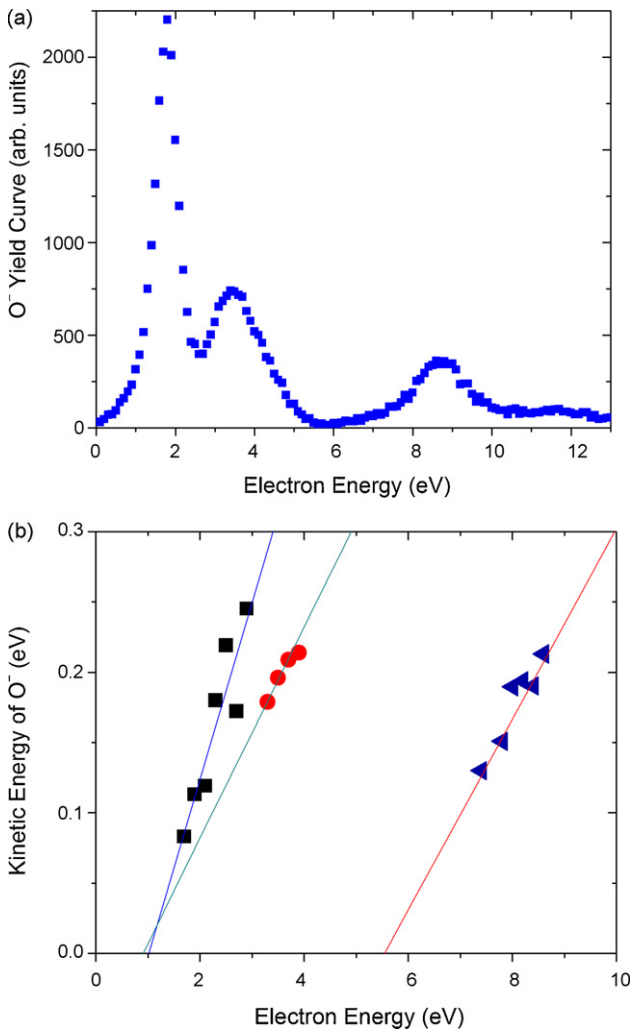

Fig. 5. O^- from DEA to NO_2. (a) Ion yield curve and (b) the measured kinetic energy as a function of electron energy across the three resonances.

below. Such a problem has been seen in earlier measurements and commented on [19].

3.2. NO_2

The DEA to NO_2 gives O^- as the dominant ion [19,20] with three main peaks located at 1.8, 3.5 and 8.5 eV, respectively, as shown in Fig. 5a. There exists no clear identification of the negative ion states corresponding to these peaks. Also no measurement has been reported on the kinetic energy of the fragment ions.

The ToF spectra of O^- from NO_2 also show only one Gaussian type peak similar to the case of O^- formation from SO_2, indicating that the ions are formed with low kinetic energy. Like in the case of SO_2, we are unable to get very accurate information due to the low kinetic energy release. However, the following qualitative features may be obtained from the data. Around all the three resonances, the width of the mass peak increases very slowly with the electron energy. The kinetic energies obtained from the ToF spectra using Eq. (4) are plotted with respect to the electron energy in Fig. 5b. For the 1.8 eV resonance, the ion kinetic energy appears to start from near zero energy indicating that the potential energy surface of the 1.8 eV resonance may have a minimum along the ON–O bond and extending into the Franck–Condon region as shown in Fig. 4. Fits for the data around the three resonances give three straight lines with very small slope. This indicates that in all the three cases, the excess energy is distributed as the internal energy of the NO fragment. The best-fit lines for the first two resonances meet the x-axis at 1 and 0.9 eV, respectively. These two are fairly close to each other considering the experimental errors and indicates same dissociation limit for the two resonances. However, this is lower than the minimum heat of formation, 1.65 eV calculated from the established thermo-chemical parameters (D(ON–O) = 3.11 eV and EA(O) = 1.46 eV). Though there could be a shift to lower energy due to the finite energy resolution of the electron beam and limitation in using Eq. (4), the difference is considerable, as in the case of SO_2.

As shown in Fig. 5b, the fitted line corresponding to the third peak at 8.5 eV gives an x-intercept of 5.6 eV. This shows that the NO is formed in an electronically excited state. The first electronically excited state of NO ($a\,^4\Pi_i$) is 4.77 eV above the ground state [17]. The corresponding threshold energy for the dissociative attachment would be 6.42 eV. Though the value obtained by us is lower by about 0.9 eV, it is consistent with the shift we observe in the dissociation limit of the first two resonances. The difference between the x-intercept between the first two resonances and the third resonance is about 4.7 eV, which is very close to the expected difference in the dissociation limits. Thus we may conclude that the third resonance may be dissociating into NO ($a\,^4\Pi_i$) + O^-.

3.3. NF_3

The DEA to NF_3 is known to give F^-, F_2^- and NF_2^- with F^- being the dominant ion. The resonance appears as a broad peak in the F^- channel with finite cross-section at zero energy, peaking at 1.8 eV and extending up to 5 eV [21]. High resolution measurements of the ion yield curve and ion kinetic energy measurements by Ruckhaberle et al. [9] have shown the broad peak to consist of two overlapping resonances centred at 1.8 and 2.2 eV, respectively. Their kinetic energy measurements for F^- indicated fairly large values. These large kinetic energies have been found to limit the accuracy of the earlier measurements on absolute DEA cross-sections on this molecule [21]. One aspect of the measurements by Ruckhaberle et al. [9] is that their plot of total ion translational energy vs. electron energy seems to give a value of −1.63 eV for ΔH_0 for the formation of F^-. Based on thermo-chemical parameters (D(F_2N–F) = 2.47 eV and EA(F) = 3.4 eV), we expect ΔH_0 to be −0.93 eV. In Fig. 6a we give the ToF spectra of F^- taken at various electron energies across the resonance along with the measured total translational energy of the fragments. Each ToF spectrum shows well-separated peaks corresponding to the 'direct' and 'turn-around' ions indicating that the ions are formed with appreciable amount of kinetic energy. The separation between the two peaks is found to increase with electron energy and above 2.2 eV an additional peak appears between the two. This additional peak indicates a new channel for the formation of F^-, but with low kinetic energy. As discussed by Ruchaberle et al. [9] this is likely to be due to the three-body fragmentation process: $F^- + F + NF$, which has an energetic threshold of 1.9 eV. Ruchaberle et al. argued that the three-body fragmentation is due to the resonance at 2.2 eV. Based on the intensities seen in the ToF spectrum, the three-body fragmentation channel seems to have relatively low cross-section as compared to the two-body process.

A plot of the kinetic energy of F^- as a function of electron energy is given in Fig. 6b. A straight line through the data points has a slope of 0.3 as against the value of 0.73, if all the excess energy appears as kinetic energy of the fragments. The smaller value indicates that considerable fraction of the excess energy being deposited into the vibrational energy of the NF_2 fragment. An extrapolation of the straight line to the x-axis provides ΔH_0 for the reaction. We find that this value is −0.92 eV, in excellent agreement with the expected value of −0.93 eV. As discussed above, the data of Ruchaberle et al. had indicated a value of −1.63 eV for ΔH_0 in this

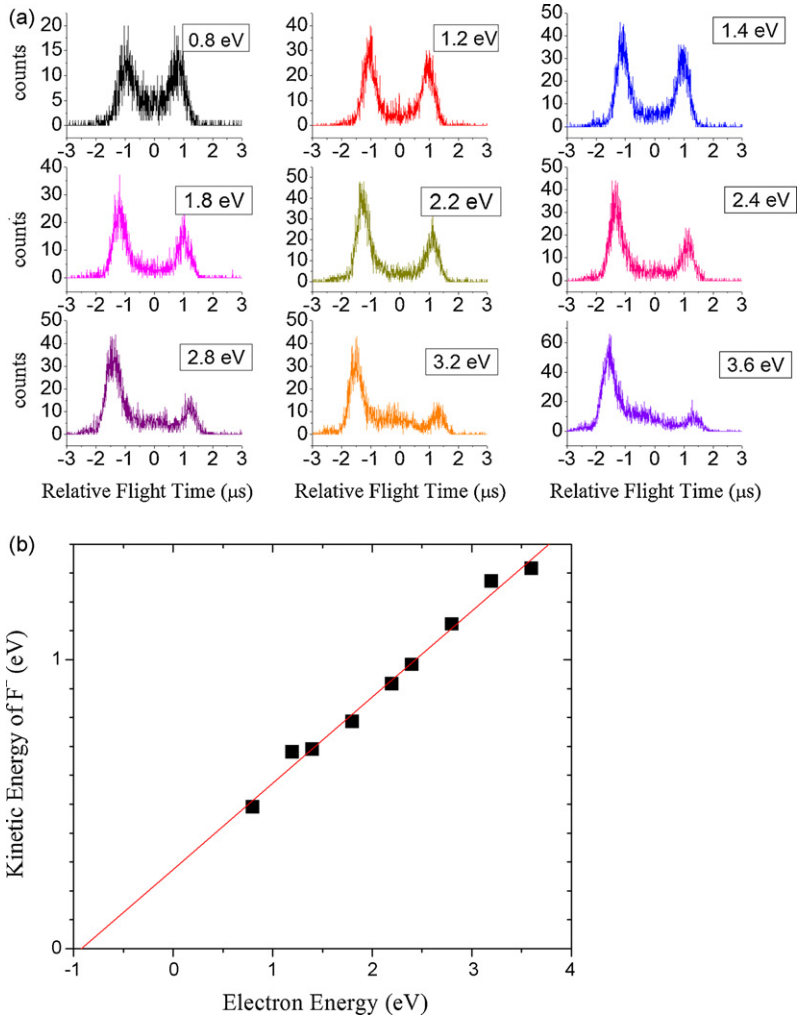

Fig. 6. F^- from DEA to NF_3. (a) Time-of-flight spectra and (b) measured kinetic energy as a function of electron energy.

case. However, we note that we have reproduced all the qualitative features of the kinetic energy measurement by Ruchaberle et al., while getting the correct threshold energy for the reaction. Again, with reference to Fig. 4, the large kinetic energy release in the two-body fragmentation channel indicates the strong repulsive nature of the potential energy surface along the F_2N–F bond in the Franck–Condon region for the two resonances.

3.4. H_2O_2

There has been only one report on DEA to H_2O_2. This provided information on the product ions, the resonances and the absolute cross-sections using two different techniques [12]. One of these employed a trochoidal electron monochromator coupled to a quadrupole mass spectrometer and the other used a simple three-element pulsed electron gun with a segmented time-of-flight spectrometer optimized for complete collection and detection of all the ions irrespective of their kinetic energy and angular distribution. In the high resolution measurements, it was found that both O^- and OH^- are produced in the ratio of 1:4 with the O^- peaking at 0.25 eV and the OH^- peaking at 0.4 eV while measurements with the experiment optimized for complete ion collection showed the combined ion yield curve of O^- and OH^- peaking at 0.6 eV. It was also found that the ion yield curve obtained using the latter technique extended beyond 2 eV. In the present ToF spectrometer also, we are unable to separate out the O^- and OH^-. However, since OH^- dominates the cross-sections, we ignore the contribution of O^- in the calculation of kinetic energy from the ToF data. The preparation of H_2O_2 to obtain a relatively pure sample in the interaction region is similar to what has been discussed earlier [12]. The ToF spectra taken at different electron energies are shown in Fig. 7. At the threshold energy, the ToF mass spectra shows one peak, fairly Gaussian in shape and no doublet structure due to 'direct' and 'turn-around' ions is seen indicating that OH^- ions are formed with very low kinetic energies. As the electron energy increases, the two peaks corresponding to the 'direct' and 'turn-around' ions start to get separated and well above the resonant peak the two peaks are separated from each other. For calculating the kinetic energy we use Eq. (2) where the ToF peaks are well separated as in the case at 1.2 and 1.4 eV. At lower energies, where the peaks are not separated, we use Eq. (4) for calculating the kinetic energy.

The kinetic energy of OH^- as a function of electron energy is shown in Fig. 7b. It is found that the kinetic energy is very small at the rising edge of the ion yield curve. This indicates that the negative ion resonance formed by electron attachment is not a purely repulsive surface, but has a minimum along the O–O bond and this extends into the Franck–Condon region as shown in Fig. 4. The DEA products start to appear when the electron energy is above the dissociation limit. We find that the ion energy increases linearly with the electron energy. The straight line through the data points has a slope of 0.45, indicating that 90% of the excess energy is going into the translational energy and that the resonance is dis-

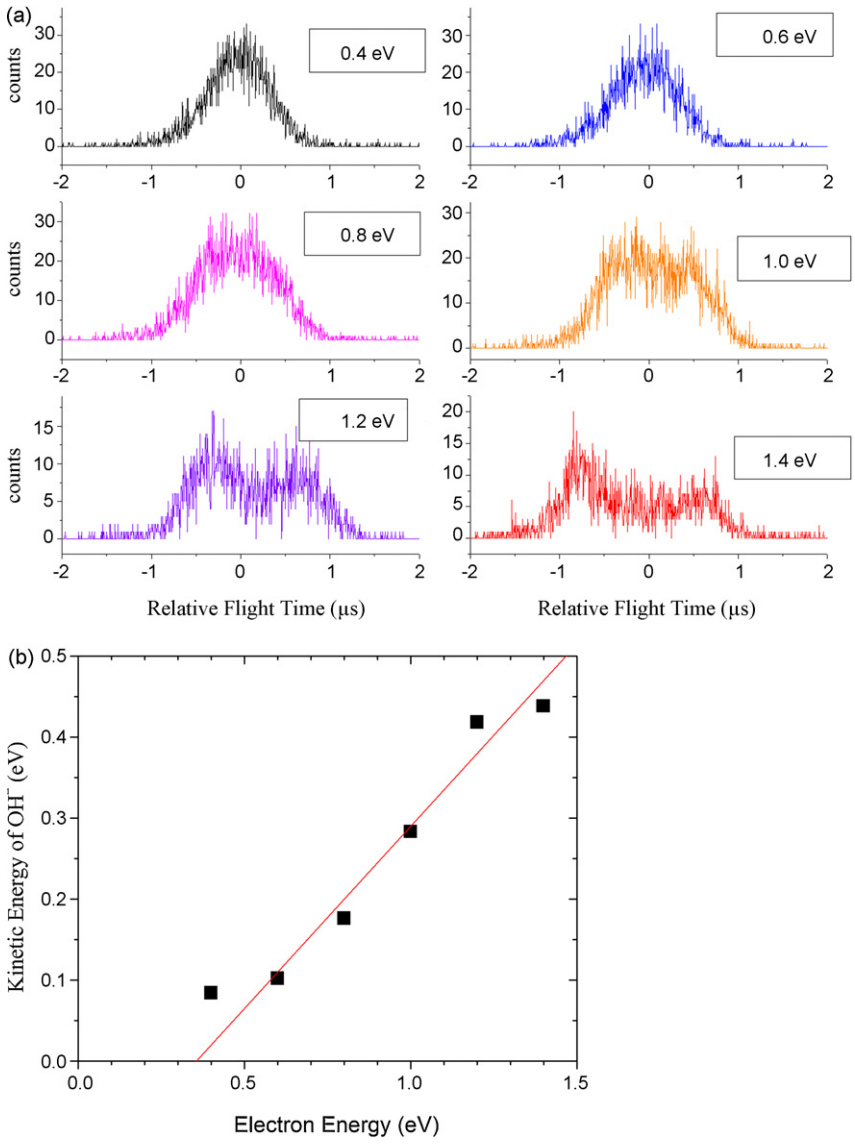

Fig. 7. OH^- from DEA to H_2O_2. (a) Time-of-flight spectra at different electron energies and (b) measured kinetic energy as a function of electron energy.

sociating almost like a diatomic system with very little vibrational excitation of the OH and OH^- fragments. An extrapolation of the straight line to electron energy axis provides the information on the appearance energy of the reaction, i.e. the electron energy that corresponds to the zero kinetic energy of the ion. The observed appearance energy (ΔH_0(obs.) = 0.35 eV) is very close to that calculated (ΔH_0(cal.) = 0.32 eV) from the established thermo-chemical parameters (D(HO–OH) = 2.15 eV, EA(OH) = 1.83 eV).

4. Conclusion

The ion kinetic energy data in the DEA to SO_2 shows that the potential energy surface of the resonance at 4.6 eV has a minimum along the OS–O bond extending into the Franck–Condon region and that most of the excess energy goes into vibrational excitation of the SO fragment as the electron energy increases. The kinetic energy of the O^- ions also shows that both the 4.6 and the 7.2 eV resonances have the same dissociation limit. In the case of NO_2 also most of the excess energy appears to be going into the vibrational excitation of the NO fragment at all the three resonances at 1.8, 3.5 and 8.5 eV, respectively. While the two lower resonances dissociates into the electronic ground state of NO, the 8.5 eV resonance appears to dissociate to give electronically excited NO ($a\ ^4\Pi_i$) state. The ion kinetic energy data also indicate that the potential energy surface of the resonance at 1.8 eV has a minimum along ON–O bond and overlapping with the Franck–Condon region. In the case of NF_3, our measurements are consistent with previous measurements by Ruchaberle et al. [9] indicating the presence of two resonances within the broad peak at 2 eV, one of which dissociates entirely through a two-body process, while the higher energy one seems to have some small probability to dissociate through a three-body process. It is also found that considerable part of the excess energy in the F^- channel goes into the internal excitation of the NF_2 fragment as observed earlier [9]. The significant difference from the earlier [9] measurements is that we have been able to obtain more reliable kinetic energy distribution for the F^- channel as seen from the excellent agreement of the measured threshold energy with the thermo-chemical data. From the kinetic energy data of OH^- from H_2O_2 we find that unlike the other three molecules discussed above, the negative ion resonance appear to dissociate almost like a diatomic system, leaving very little internal energy in the OH and OH^- fragments and that the potential energy surface of the resonance has a minimum along the O–O bond and it extends into the Franck–Condon region.

References

[1] V.S. Prabhudesai, A.H. Kelkar, D. Nandi, E. Krishnakumar, Phys. Rev. Lett. 95 (2005) 143202.
[2] S. Ptasinska, S. Deniff, V. Grill, T.D. Mark, E. Illenberger, P. Scheier, Phys. Rev. Lett. 95 (2005) 093201.
[3] T. Jaffke, R. Hashemi, L.G. Christophorou, E. Illenberger, H. Baumgartel, Chem. Phys. Lett. 203 (1993) 21.
[4] E. Krishnakumar, S.V.K. Kumar, S.A. Rangwala, S.K. Mitra, Phys. Rev. A 56 (1997) 1945.
[5] S.V.K. Kumar, V.S. Ashoka, E. Krishnakumar, Phys. Rev. A 70 (2004) 052715.
[6] K.E. Greenberg, J.T. Verdeyen, J. Appl. Phys. 57 (1985) 1596.
[7] J. Perrin, J. Meot, J.-M. Seifert, J. Schmitt, Plasma Chem. Plasma Processing 10 (1990) 571.
[8] H. Reichardt, A. Frenzel, K. Schober, Microelectron. Eng. 56 (2001) 73.
[9] N. Ruchaberle, L. Lehman, S. Matejcik, E. Illenberger, Y. Bouteiller, V. Periquet, L. Museur, C. Desfrancois, J.-P. Schermann, J. Phys. Chem. 101 (1997) 9942.
[10] P.J. Crutzen, J. Fishman, Geophys. Res. Lett. 4 (1977) 321.
[11] J.K. Thomas, in: M. Burton, J.L. Magee (Eds.), Elementary Processes and Reactions in the Radiolysis of Water, Advances in Radiation Chemistry, vol. 1, Wiley Interscience, New York, London, 1969, pp. 103–198.
[12] D. Nandi, E. Krishnakumar, A. Rosa, W.-F. Schmidt, E. Illenberger, Chem. Phys. Lett. 373 (2003) 454.
[13] E. Illenberger, Chem. Phys. Lett. 80 (1981) 153.
[14] P.W. Harland, J.L. Franklin, J. Chem. Phys. 61 (1974) 1621.
[15] D. Rapp, D.D. Briglia, J. Chem. Phys. 63 (1965) 1480.
[16] E. Krishnakumar, S.V.K. Kumar, S.A. Rangwala, S.K. Mitra, J. Phys. B 29 (1996) L657.
[17] K.P. Huber, G. Herzberg, Constants of Diatomic Molecules, Series: Molecular Spectra and Molecular Structure, vol. 4, Van Nostrand, New York, 1979.
[18] R. Abouaf, F. Fiquet-Fayard, J. Phys. B 9 (1976) L323.
[19] R. Abouaf, R. Paineau, F. Fiquet-Fayard, J. Phys. B 9 (1976) 303.
[20] S.A. Rangwala, E. Krishnakumar, S.V.K. Kumar, Phys. Rev. A 68 (2003) 052710.
[21] D. Nandi, S.A. Rangwala, S.V.K. Kumar, E. Krishnakumar, Int. J. Mass Spectrom. 205 (2001) 111.